

## Dipolar Defect Model for Fatigue in Ferroelectric Perovskites

S. Pöykkö and D. J. Chadi

NEC Research Institute, 4 Independence Way, Princeton, New Jersey 08540

(Received 4 December 1998)

A microscopic model for polarization fatigue in ferroelectric perovskites based on dipolar defects formed by the combination of oxygen vacancies and impurity metal ions is presented. The binding energy of an oxygen vacancy to a Pt impurity in  $\text{PbTiO}_3$  is calculated to be  $\sim 2.9$  eV. The complex is strongly polar, is stabilized by electron capture, and pins the polarization of the surrounding lattice.

PACS numbers: 77.84.Dy

Ferroelectric (FE) materials have been extensively studied in recent years because of their promising properties for nonvolatile random access memories as well as several other applications [1]. There are, however, serious material-related problems hampering the widespread use of ferroelectrics. Perhaps the most severe ones are fatigue, which is the decrease in the amount of switchable polarization after repeated (e.g.,  $10^8$ – $10^{10}$ ) polarization reversals, and imprint, in which after extended poling one polarization direction becomes preferred over the other. Both of these can lead to read errors of the logical state of a memory cell. Despite extensive studies, a satisfying explanation for fatigue and imprint is still lacking. Perovskite ferroelectrics, especially lead zirconate titanate (PZT), represent an important class of FE materials. PZT capacitors with simple metal (such as Pt) electrodes (Pt/PZT/Pt) are compatible with silicon technology, but their fatigue resistance is poor. Some layered perovskite oxides, such as  $\text{SrBi}_2\text{Ta}_2\text{O}_9$  [2] and PZT capacitors with metal oxide electrodes, show superior fatigue resistance as compared to Pt/PZT/Pt capacitors, but generally require higher processing temperatures and are not usually compatible with silicon technology.

Auger microprobe data of Scott *et al.* [3] show that, in PZT capacitors with platinum electrodes, a high concentration of Pt and a deficiency of oxygen in PZT films occur simultaneously in fatigued regions. Warren *et al.* [4] find that the electron paramagnetic resonance (EPR) signal from Pt increases with fatigue in  $\text{BaTiO}_3$ . From analysis of their data, they suggest a fatigue-induced lattice distortion that is stabilized by electron trapping on Pt, possibly involving a nearby oxygen vacancy ( $V_{\text{O}}$ ). They also find that the fatigue-induced trapped electron is both thermally and electrically stable.

In this Letter we report on our studies of the properties of oxygen-vacancy Pt metal-impurity defect complexes in  $\text{PbTiO}_3$ . The results are expected to be qualitatively the same for other simple ferroelectric perovskites in which a complexing of a donorlike defect such as  $V_{\text{O}}$ , and an acceptorlike impurity, results in a highly polar complex. The large concentration of metallic acceptor impurities in PZT may cause an accumulation of impurity-vacancy complexes and thus suppress the switchable polarization.

Polarization pinning by defects was observed in the case of Mn-doped  $\text{BaTiO}_3$  by Lambeck and Jonker in the 1970s [5].

The oxygen-vacancy–metal-impurity defect is a dipolar complex that may be formed in the following process: a substitutional impurity metal atom, e.g., Pt, traps one or two electrons thus changing its ionization state from 4+ to either 3+ or 2+. Once an oxygen vacancy and Pt atom move close to each other, the strong interaction between them leads to the creation of a highly polar defect pair. Polarization inversions speed up oxygen-vacancy diffusion and more defect dipoles are formed. Schematic models for some possible defects created in this type of process are shown in Fig. 1.

We have calculated the electronic and ionic structures for the defects shown in Fig. 1 using a first-principles total energy method. Our plane-wave pseudopotential calculations are based on the density functional theory (DFT) within local density approximation [6]. Methods based on the DFT have been successfully applied to

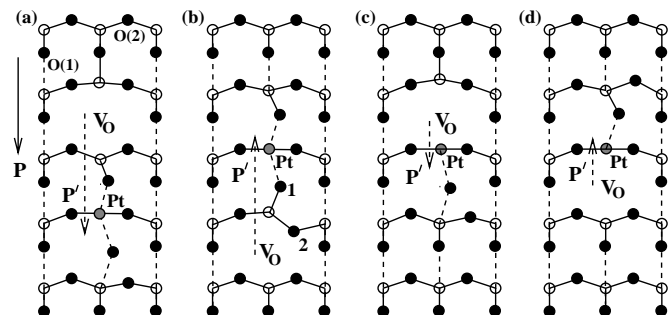


FIG. 1. Schematic models for next-nearest- [(a), (b)] and nearest-neighbor [(c), (d)]  $\text{Pt}_{\text{Ti}}\text{V}_{\text{O}(1)}$  defect pairs. Only atoms on the same plane as the vacancy and impurity atoms are shown. The solid circles represent oxygen and the open circles represent titanium atoms. Lead atoms are not in the plane of the figures and are not shown. Characteristic atomic relaxations are shown in all cases. The most significant atomic relaxations take place in a single  $bc$  plane as shown in (a)–(d).  $\mathbf{P}$  (solid line) and  $\mathbf{P}'$  (dashed line) are the directions of bulk and defect polarizations, respectively. In (a) and (c), defect polarization is in the same direction as the bulk polarization ( $+\mathbf{P}'$ ), and in (b) and (d) the defect polarization ( $-\mathbf{P}'$ ) is in the opposite direction.

ferroelectric materials to explain microscopic mechanisms of spontaneous polarization [7,8] and phase diagrams [9,10]. Norm-conserving nonlocal [11] Troullier–Martins-type [12] pseudopotentials for Pb, Ti, O, and Pt are used. The semicore states of Pb ( $5d$ ) and Ti ( $3p$ ) were treated as core states, but nonlinear core valence corrections [13] were employed to improve transferability of the generated pseudopotentials. The  $s$  component was treated as a local one and these pseudopotentials were tested and shown to be ghost free [14]. The energy cutoff for the plane-wave expansion used in the calculation was 39 Ry. The Brillouin zone sampling was done by a  $2 \times 2 \times 1$  Monkhorst-Pack  $\mathbf{k}$ -point mesh [15] for an 80 atom ( $2a \times 2a \times 4c$ ) supercell. The calculated lattice constant for the cubic phase is 3.94 Å, which is about 1% smaller than the experimental one [16]. The energy reduction in the phase transition from the cubic to the tetragonal phase is calculated to be 0.24 eV per 5 atom unit cell. These numbers are in good agreement with previous studies [8,17]. In our calculations all atoms closer than  $\sim 6$  Å from a defected lattice site have been allowed to relax from their optimized bulk positions without any symmetry assumptions.

The bonding in  $\text{PbTiO}_3$  is mostly ionic with the covalent contribution being most important in describing Ti-O bonds. It is worth noting that despite the complicated bonding even a simple electrostatic model has been successful in explaining atomic ordering in complex perovskite alloys [18]. In the tetragonal phase there are two types of oxygen atoms: oxygen atoms bonded to two Ti atoms in  $ab$  planes [O(2) in Fig. 1(a)], and O atoms in O-Ti-O chains in the  $c$ -direction [O(1) in Fig. 1(a)] with short and long bonds. This latter bonded/decoupled Ti-O pattern is the microscopic origin of the macroscopic polarization.

The microscopic factors that cause a suppression of the switchable polarization (i.e., fatigue) have to be energetically very strong. This means that the atomic scale processes causing fatigue should have a very clear fingerprint in their energetics and should be highly exothermic. Unlike formation energies, binding energies  $E_B$  (defined as the energy released in the formation of a pair from its isolated components) are readily obtainable from the supercell energies for the isolated defects [ $E_{D1}(Q_1)$  and  $E_{D2}(Q_2)$ ], for the defect pair  $E_P(Q_P)$ , and for the bulk ( $E_{\text{bulk}}$ ):

$$E_B = E_P(Q_P) + E_{\text{bulk}} - E_{D1}(Q_{D1}) - E_{D2}(Q_{D2}) + (Q_P - Q_{D1} - Q_{D2})(\mu_e + E_{\text{VBM}}), \quad (1)$$

where  $Q$  denotes the defect charge,  $\mu_e$  is the electron chemical potential, and  $E_{\text{VBM}}$  is the energy of the valence band maximum. This energy difference has to be calculated between the most stable charge states for each value of  $\mu_e$ . Calculated binding energies  $E_B$  for nearest-neighbor pairs are shown in Fig. 2. The stable charge states for most values of the electron chemical potential

for  $V_{\text{O}(1)}$  and  $\text{Pt}_{\text{Ti}}$  are  $2+$  and  $0$ , respectively. Therefore, pairing of  $V_{\text{O}(1)}$  and  $\text{Pt}_{\text{Ti}}$  would result in a doubly positive defect. However, a doubly positive nearest-neighbor  $\text{Pt}_{\text{Ti}}V_{\text{O}(1)}$  pair is not stable. Electron trapping is essential to the stabilization of the pair. For neutral charge states of  $\text{Pt}_{\text{Ti}}V_{\text{O}(1)}$ , optimal values of the binding energies are extremely large: 1.3 eV when the defect polarization is in the same direction as the bulk polarization [denoted by  $+P'$ , Fig. 1(c)] and 2.9 eV for opposite bulk and defect polarizations [denoted by  $-P'$ , Fig. 1(d)].

The large preference of  $-P'$  over  $+P'$  indicates that the nearest-neighbor  $\text{Pt}_{\text{Ti}}V_{\text{O}(1)}$  defect is effectively a polarization pinning center, not only by having a net polarization itself but also by forcing the polarization in the surrounding O-Ti-O chains to be in an opposite direction to its own polarization axis. The 1.6 eV energy difference between the two defect polarization configurations is large, as compared, for example, to the 0.24 eV energy gain per five-atom unit cell in the phase transition from the cubic to the tetragonal phase. As more and more polarization inversions take place the number of pairs increases since an external electric field accelerates vacancy diffusion and thus increases the probability for pair formation. This leads to a rapid decrease in the switchable polarization, because each newly created defect freezes the polarization in some additional volume of the crystal. Since a complex freezes its surrounding bulk region in an *opposite* polarization state to its own dipole moment, the presence of impurity-vacancy complexes may not necessarily induce voltage shifts (i.e., a preference of one polarization direction over another) even in the case where a majority of defect complexes have the same polarization direction. However, by freezing the

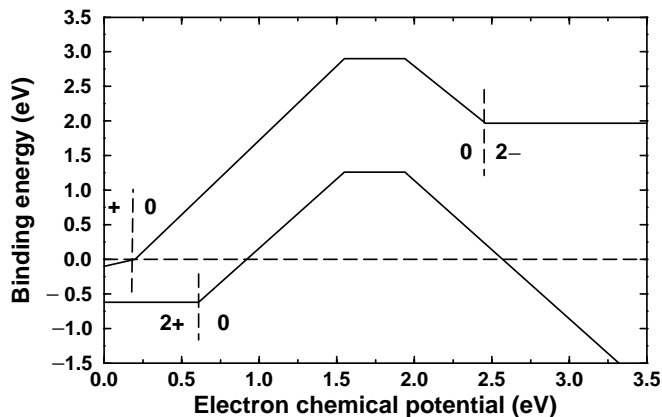


FIG. 2. Binding energy as a function of electron chemical potential ( $\mu_e$ ) for nearest-neighbor  $\text{Pt}_{\text{Ti}}V_{\text{O}(1)}$  defect pairs. Vertical dashed lines represent values of  $\mu_e$ , where the most stable charge state of the pair changes from that shown on the left to that indicated on the right-hand side of the dashed line. Kinks in the solid lines at 1.6 and 2.0 eV are, correspondingly, due to the changes in the most stable charge states of  $\text{Pt}_{\text{Ti}}$  ( $0/2-$ ) and  $V_{\text{O}(1)}$  ( $2+/0$ ). The horizontal dashed line represents zero binding energy. A doubly positive  $\text{Pt}_{\text{Ti}}V_{\text{O}(1)}$  ( $+P'$ ) defect pair is unstable towards dissociation to isolated vacancy and Pt impurity.

polarization, vacancy-impurity pairs introduce pinned regions which do not contribute to the macroscopic polarization. The fact that the stability of a  $\text{Pt}_{\text{Ti}}V_{\text{O}(1)}$  pair is due to electrons trapped on the center explains why electron injection is more crucial to fatigue than hole injection [19].

The calculated binding energies for  $\text{Pt}_{\text{Ti}}V_{\text{O}(1)}$  are far too large to originate merely from Coulombic attraction. The major part of the binding energy comes from atomic relaxations and rebonding in the vicinity of  $V_{\text{O}(1)}$  and  $\text{Pt}_{\text{Ti}}$ . Isolated, doubly negative  $\text{Pt}_{\text{Ti}}$  causes very strong relaxations in the neighboring lattice. The symmetry of the defect is lowered as a result of relaxation. The strongest effect is on the nearest-neighbor oxygen atoms in the  $c$  direction; these atoms move far away from Pt to an almost interstitial position between two lead atoms. The relaxation is larger for the oxygen atom bonded to Pt in the unrelaxed structure; this O atom moves by  $\sim 0.7$  Å into the  $ab$  plane of Pb atoms. In the neutral charge state the lattice relaxations around  $\text{Pt}_{\text{Ti}}$  are similar but much smaller. The platinum impurity atom itself moves in both charge states so that it is in the same  $ab$  plane as the type-2 oxygen atoms [O(2)]. The stability of doubly negative charge state is strongly enhanced by relaxations; the relaxation energy is 1.9 eV for  $2-$  charge state and only 0.6 eV for neutral charge state. According to our calculations a singly negative charge state of isolated Pt impurity is unstable by 0.25 eV (i.e., it is a negative  $U$  center). This result is in agreement with EPR experiments of Warren *et al.* [4]; they find that, in unfatigued  $\text{BaTiO}_3$  samples, EPR active Pt centers can only be metastably created by low temperature band gap illumination.

For an isolated doubly positive oxygen vacancy the relaxations can be understood in terms of Coulombic interactions: the nearest two Ti and four Pb cations are displaced away from  $V_{\text{O}(1)}$  and the nearest eight O anions are attracted towards it [17]. The most important relaxation is for the nearest-neighbor Ti atom which was bonded to the missing oxygen atom. This atom moves ( $\sim 0.4$  Å) along the  $c$  axis to the opposite side of the  $ab$  plane of type-2 oxygen atoms [O(2)]. The relaxations around neutral  $V_{\text{O}(1)}$  are similar but smaller in magnitude. Relaxations enhance the stability of doubly positive vacancy over the neutral one by 2.2 eV.

The large atomic movements in the relaxations of the  $\text{Pt}_{\text{Ti}}^{2-}$  and  $V_{\text{O}(1)}^{2+}$  cause strain in the back bonds. For defect complexes, relaxations are smaller than for isolated vacancies or impurities; thus strain for the back bonds is reduced and energy is reduced (i.e., the binding energy is increased).

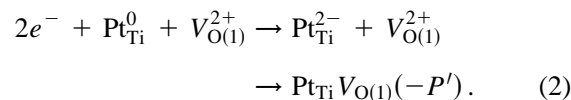
The most important factor contributing to the large binding energy for the nearest-neighbor  $\text{Pt}_{\text{Ti}}V_{\text{O}(1)}$  pair is that, since the Pt impurity is missing one of its neighboring oxygen atoms, it does not have to spend any energy to push it away from itself. The big preference of  $-P'$  [Fig. 1(d)] over  $+P'$  [Fig. 1(c)] is due to the following effects. First,

in the case of  $-P'$  the fact that Pt stabilizes itself to the  $ab$  plane of oxygen atoms moves it in the direction that  $V_{\text{O}(1)}$  would push it (away from the vacancy center), whereas in the case of  $+P'$  these effects compete. Second, the missing oxygen atom in the case of  $-P'$  is the oxygen atom for which the relaxation is largest, which further increases the energy preference.

The trapped electron causes a distortion of the oxygen tetrahedra surrounding a Pt atom [Figs. 1(c) and 1(d)] and the trapping is stabilized by a nearby oxygen vacancy, which is exactly what Warren *et al.* [4] have seen in the case of  $\text{BaTiO}_3$ . There is also a narrow electron chemical potential window for which a singly negative (EPR active) charge state is the most stable one. This is in contrast to an isolated Pt impurity which does not have a stable EPR active charge state. This is in agreement with EPR results of Warren *et al.* [4]. They find that EPR active Pt impurity center ( $\text{Pt}_{\text{Ti}}V_{\text{O}(1)}$ ) in fatigued  $\text{BaTiO}_3$  is stable while in the unfatigued samples (isolated Pt impurities), the EPR active state is only metastable.

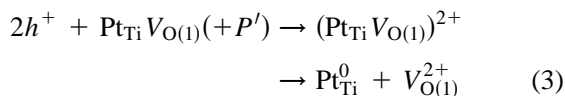
The binding energy is low (0.1 eV  $+P'$ , 0.6 eV  $-P'$ ) for a next-nearest-neighbor  $\text{Pt}_{\text{Ti}}V_{\text{O}(1)}$  pair [Figs. 1(a) and 1(b)]. Most of the calculated binding energy comes from the relaxation of the oxygen atoms marked as 1 and 2 in Fig. 1(b). These relaxations clearly show a tendency for vacancy diffusion from a type-1 next-nearest-neighbor [ $V_{\text{O}(1)}$ ] site to the type-2 nearest-neighbor [ $V_{\text{O}(2)}$ ] site, which in turn is unstable for a relaxation into a nearest-neighbor type-1 structure [Fig. 1(d)].

The calculated binding energies can be used to calculate energies for possible chemical reactions. In the presence of mobile electronic charge the vacancy-impurity defect may be created by the following chemical reaction:



The energy released in this process is 3 eV. The charge states in the above process are defect charges.

It is difficult to dissociate the defect complex since the electronic level occupied by electrons trapped on  $\text{Pt}_{\text{Ti}}V_{\text{O}(1)}$  ( $-P'$ ) lies below the valence band maximum (VBM). In contrast, in the case of  $+P'$ , this electronic level is in the band gap. In order to dissociate the complex, either 3 eV energy is needed or the defect and the surrounding lattice polarization have to first become aligned, allowing the complex to lose its trapped electrons (they may recombine with mobile holes if holes are present) and finally the complex can dissociate. A defect and its surrounding lattice polarization may become aligned ( $+P'$ ) under a strong poling field and the electronic level occupied by the trapped charge rises simultaneously to the band gap. If mobile holes are present dissociation of the complex via the chemical reaction



would release 0.6 eV energy per complex. The reactions in Eqs. (2) and (3) offer an alternative explanation for the observed optically and thermally induced suppression of switchable polarization and corresponding recoveries of it [20]. In the experiments of Warren *et al.* [20], PZT samples are either illuminated by band gap light or heated to 100 °C while applying a bias voltage just below the switching threshold. Fatigued samples may be restored by applying a full switching bias in the opposite direction while illuminating or heating the samples. Optical and thermal fatigue is strongly dependent on the applied voltage; no suppression is reported for either zero or full switching voltage [20]. There is also direct experimental evidence for oxygen-vacancy-related defect dipole alignment via a heat/bias combination in the case of BaTiO<sub>3</sub> [21]. Our explanation for these effects is as follows: both illumination and heating produce mobile charge carriers (electrons and holes). The effect of a small voltage is to speed up the diffusion of charged defects. Because mobile electrons are now available, the process in Eq. (2) takes place and the polarization is suppressed. As the bias voltage is increased it forces more and more effectively the alignment of defect and bulk polarizations, and thus the electronic state of the Pt<sub>Ti</sub>V<sub>O(1)</sub> defect rises into the band gap and emptying it becomes possible. Again mobile charge carriers, specifically holes, are available and the reaction in Eq. (3) takes place and switchable polarization is recovered. The polarization depinning by applied voltage was originally discovered by Scott and Pouligny [22].

Warren *et al.* [20] also found that the switchable polarization is only partially recovered if the bias voltage is not reversed after illumination/bias (or heat/bias) treatment. This is also understandable in the terms of vacancy-impurity pairs. During the illumination/bias (or heat/bias) treatment, most of the pairs created are oriented in such a way that the forces due to the external field acting on the vacancy and the impurity push them closer to each other. Therefore separation of pairs requires their reorientation (i.e., diffusion of V<sub>O</sub> and/or Pt<sub>Ti</sub>). Because dipolar defects are slow to reorient, the recovery is only partial. If the direction of the bias voltage is reversed, the electric field causes a drift of the vacancy and impurity ends of the complex away from each other, and no defect reorientation is needed to break pairs, resulting in a fast and complete recovery of the switchable polarization.

In summary, we have shown that oxygen-vacancy-platinum-impurity pairs are tightly bound dipolar defects, which may cause a suppression of switchable polarization. The calculated binding energies are large enough to prevent dissociation of the complexes by an electric field. The better fatigue performance of metal oxide electrodes over simple metal electrodes may arise not solely because oxides can act as a sink for oxygen vacancies, but also from a decrease in the diffusion of metal atoms into PZT films. Fatigue resistance should also improve by decreasing the acceptor impurity concentrations in PZT films.

- 
- [1] See, for example, J.F. Scott, *Ferroelectrics Rev.* **1**, 1 (1998).
  - [2] C. A-Paz de Araujo *et al.*, *Nature (London)* **374**, 627 (1995).
  - [3] J.F. Scott *et al.*, *J. Appl. Phys.* **70**, 382 (1991).
  - [4] W.L. Warren *et al.*, *Appl. Phys. Lett.* **67**, 1426 (1995).
  - [5] P.V. Lambeck and G.H. Jonker, *Ferroelectrics* **22**, 729 (1978).
  - [6] R. O. Jones and O. Gunnarson, *Rev. Mod. Phys.* **61**, 689 (1989).
  - [7] R.D. King-Smith and D. Vanderbilt, *Phys. Rev. B* **47**, 1651 (1993); **49**, 5828 (1994); D. Vanderbilt and R.D. King-Smith, **48**, 4442 (1993).
  - [8] R.E. Cohen, *Nature (London)* **358**, 136 (1992); R.E. Cohen and H. Krakauer, *Phys. Rev. B* **42**, 6416 (1990).
  - [9] W. Zhong *et al.*, *Phys. Rev. Lett.* **72**, 3618 (1994); **73**, 1861 (1994).
  - [10] U.V. Waghmare and K.M. Rabe, *Phys. Rev. B* **55**, 6161 (1997).
  - [11] L. Kleinman and D.M. Bylander, *Phys. Rev. Lett.* **48**, 1425 (1982).
  - [12] N. Troullier and J.L. Martins, *Phys. Rev. B* **43**, 1993 (1991).
  - [13] S.G. Louie *et al.*, *Phys. Rev. B* **26**, 1738 (1982).
  - [14] X. Gonze *et al.*, *Phys. Rev. B* **41**, 12 264 (1990); X. Gonze *et al.*, *Phys. Rev. B* **44**, 8503 (1991).
  - [15] H.J. Monkhorst and J.D. Pack, *Phys. Rev. B* **13**, 5188 (1976).
  - [16] *Landolt-Börnstein Tables*, edited by K.-H. Hellwege and A. M. Hellwege (Springer, Berlin, 1969).
  - [17] C.H. Park and D.J. Chadi, *Phys. Rev. B* **57**, 13961 (1998).
  - [18] L. Bellaiche and D. Vanderbilt, *Phys. Rev. Lett.* **81**, 1318 (1998).
  - [19] X. Du and I.-W. Chen, *J. Appl. Phys.* **83**, 7789 (1998).
  - [20] W.L. Warren *et al.*, *J. Appl. Phys.* **77**, 6695 (1995).
  - [21] W.L. Warren *et al.*, *Appl. Phys. Lett.* **67**, 1689 (1995).
  - [22] J.F. Scott and B. Pouligny, *J. Appl. Phys.* **64**, 1547 (1988).